

# Numerical Studies on Flow characteristics Past A Cavity With Spoiler Relating Velocity Field And OASPL Through LES Approach

**Dr. Nirmal Kumar Kund**

Associate Professor, Dept of Production Engineering  
Veer SurendraSai University of Technology, Burla, Odisha, India

**Abstract-** *The current study encompasses the development of a suitable numerical model concerning the supersonic flow past a three-dimensional open cavity with length-to-depth ratio of 2. The Mach number of the supersonic free-stream is 2 in addition the Reynolds number of the flow is  $10^5$ . The numerical simulations have been accomplished through the Large Eddy Simulation (LES) practice. The Smagorinsky model is introduced for this research. The simulation results have been obtained in the form of pressure field as well as overall sound pressure level at the centreline of the aft wall of the open cavity. Quite large recirculation is also witnessed within the open cavity without spoiler. But, the reduction of the recirculation within the open cavity is accomplished by attaching a spoiler in the form of one-fourth of a cylinder at the leading edge of the open cavity. With the attachment of the spoiler, the overall sound pressure level at the centreline of the aft wall of the open cavity is also decreased to some amount. Alongside, the sound pressure level is suppressed by almost 14 dB and 18 dB at both front and aft walls of the open cavity. The variations in the flow structures of the open cavity flow attaching the spoiler is also examined with the velocity vectors. In general, the comparisons between the simulation predictions of the cavity flows with and without the attachment of the spoiler is also ascertained.*

**Keywords-** Numerical Simulation, Open Cavity, Spoiler, LES, Velocity Vector, OASPL.

## I. INTRODUCTION

The flow induced noise is very pragmatic in our day-to-day life such as in exhaust pipes, vacuum cleaners, ventilation systems, fans etc. The flow induced noise is the greatest ever challenge in many engineering practices concerning surface transport, aviation and marine applications. Airframe noise is the noteworthy component of overall noise. One of the most imperative airframe noises is the cavity noise. It is created from open wheel wells, weapon bays, door gaps, side mirrors, open sun roof, etc. The door gaps, wheel wells and weapon bays may be modelled as rectangular cavities and

the collected flow outside the cavity may be taken to be uniform and smooth. Even if the rectangular cavity is simple in shape, it is very rich in diverse dynamic as well as acoustic sensations, usually enclosed by an aeroacoustic feedback loop pertaining to the shape/size of the cavity over and above the flow circumstances. Quite severe tone noises can be produced on account of the vortex shredding at the upstream edge of the cavity during the flow over a cavity.

## II. LITERATURE REVIEW

The flow-induced pressure oscillations in shallow cavities are described by Heller et al. [1]. The investigations on the tones and pressure oscillations induced by flow over rectangular cavities are carried out by Tam and Block [2]. Mach 0.6 to 3.0 flows over rectangular cavities are performed by Kaufman et al. [3]. The high resolution schemes are used by Sweby [4] in applying flux limiters on hyperbolic conservation laws. The numerical simulation on supersonic flow over a 3D cavity are reported by Rizzetta [5]. The very fundamentals of computational fluid dynamics is demonstrated by Anderson and Wendt [6]. The achievements and challenges of large-eddy simulation are described by Piomelli [7]. The numerical simulations of fluidic control for transonic cavity flows are carried out by Hamed et al. [8]. The LES studies on feedback-loop mechanism of supersonic open cavity flows are conducted by Li et al. [9]. A validation study on unsteady RANS computations of supersonic flow over 2D cavity is done by Vijayakrishnan [10]. The lid-driven cavity flows of viscoelastic liquids are very well illustrated by Sousa et al. [11]. The experimental investigations on double-cavity flows are studied by Tuerke et al. [12]. It is noticed that a comprehensive study on cavity flow has been accomplished both experimentally as well as numerically for improving the aerodynamic effectiveness. On the other hand, despite its distinction, the complex flow physics of flow over a cavity has enchanted the investigators around the globe for further researches and yet remains to be a frontier area of research.

### III. OBJECTIVES OF PRESENT RESEARCH WORK

Even though, ample experiments have been conducted to quash the recirculation within the cavity, but, several are not just effective for all flow circumstances. The operation of the control devices are very portentously influenced by the Mach number. Control devices require to be appropriately designed so that they perform over a wide range of Mach numbers. The incoming boundary layer is also one more vital factor which controls the operation of the control devices. Emphasising this perspective in mind, the motivation of this investigation is to examine the flow sensation in a 3D open cavity supersonic flow. Furthermore, the reduction of recirculation within the open cavity by passive technique has been investigated by attaching spoiler at the leading edge of the cavity. The comparison between the open cavity flows with and without the attachment of spoiler has also been made. In general, the current researches involve the establishment of a three-dimensional numerical model for absolute numerical predictions of the open cavity flows in terms of velocity vector and overall sound pressure level (OASPL) at the centreline of the aft wall of the open cavity with and without the attachment of the spoilers.

### IV. DESCRIPTION OF PHYSICAL PROBLEM

Supersonic flow past a three-dimensional cavity is studied numerically. The streamwise length, depth and spanwise length of the cavity are 20 mm, 10 mm, and 10 mm, respectively. The length-to-depth ratio ( $L/D$ ) for the cavity is 2. The width-to-depth ratio ( $W/D$ ) is 1. The cavity is three-dimensional with streamwise length-to-spanwise length ratio ( $L/W$ ) > 1. In addition, the Mach number of the free-stream along with the Reynolds number based on the cavity depth are taken as 2 and  $10^5$ , respectively, for setting the inflow conditions.

#### A. Geometric model

The computational domain of the cavity with the spoiler is shown in figure 1. The size of this domain, as stated previously, is  $2D \times D \times D$  (length  $\times$  depth  $\times$  width). The spoiler at the cavity leading edge has a dimension of  $0.6D$ . One-fourth part of a cylinder has been used for the shape of the spoiler. The domain is three-dimensional with  $L/W > 1$ . The upper boundary is at a distance of  $4D$  above the cavity to ensure that no reflected shock affects the flow features inside the cavity.

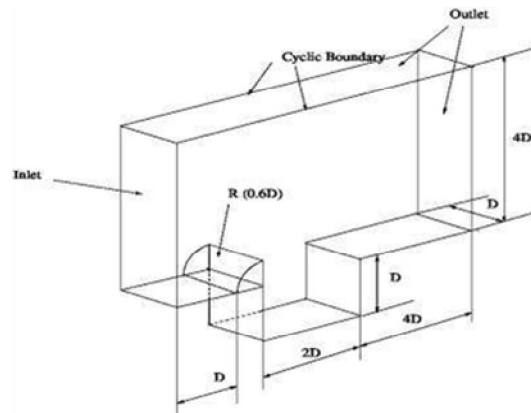


Figure 1. Computational domain of cavity with spoiler

#### B. Initial and boundary conditions

The initial conditions for the cavity involving supersonic flow are Mach number = 2 with  $P_\infty = 101.325 \text{ kPa}$  and  $T_\infty = 300 \text{ K}$  at the inlet, Reynolds number of the flow being 105, based on the cavity depth.

No-slip adiabatic wall boundary conditions are applied at the wall boundaries. Zero-gradient condition is applied at all the out flow boundaries. Periodical boundary condition is applied in the span wise direction of the cavity. No-slip adiabatic wall boundary condition is employed for the spoiler.

### V. MATHEMATICAL FORMULATION

#### A. Generalized governing transport equations

The 3D compressible Navier-Stokes equations are the governing equations which comprise the continuity equation (1), the momentum equation (2), and the energy equation (3) which are as mentioned below:

$$\frac{\partial \rho}{\partial t} + \nabla \cdot (\rho \mathbf{U}) = 0 \tag{1}$$

$$\frac{\partial (\rho \mathbf{U})}{\partial t} + \nabla \cdot (\rho \mathbf{U} \cdot \mathbf{U}) - \nabla \cdot (\mu \nabla \mathbf{U}) = -\nabla p \tag{2}$$

$$\frac{\partial (\rho e)}{\partial t} + \nabla \cdot (\rho e \mathbf{U}) - \nabla \cdot (\mu \nabla e) = -p(\nabla \cdot \mathbf{U}) + \mu \left[ \frac{1}{2} (\nabla \mathbf{U} + \nabla \mathbf{U}^T) \right]^2 \tag{3}$$

Where,

$$\mathbf{U} = \text{velocity vector} = u\mathbf{i} + v\mathbf{j} + w\mathbf{k}$$

$$\frac{1}{2} (\nabla \mathbf{U} + \nabla \mathbf{U}^T) = \text{strain rate tensor.}$$

The equations (1), (2) and (3) symbolise the conservation form of the Navier-Stokes equations. The conservation form of these governing equations are reached

from a flow model fixed in space [6]. The stated equations are relevant to viscous flow, except that the mass diffusion is not involved.

It is supposed, in aerodynamics, that the gas is a perfect gas. The equation of state for a perfect gas is,  $p = \rho RT$

$$(4)$$

Where,  $R$  = specific gas constant =  $C_p - C_v$

$$(5)$$

For a calorically perfect gas (constant specific heats), the caloric equation of state is,

$e$  = internal energy per unit mass =  $C_v T$

$$(6)$$

### B. LES turbulence modeling

The turbulent flows may be simulated applying three different methods: Reynolds-Averaged Navier-Stokes equations (RANS), direct numerical simulation (DNS), and large eddy simulation (LES). Direct numerical simulation has high computational necessities. DNS resolves all the scales of motion and for this it desires a number of grid points proportional to  $(Re)^{9/4}$  and computational scales' cost is proportional to  $(Re)^3$  [7].

In the current investigation, behaviours of the turbulent flow field have been simulated applying LES as it is suitable for unsteady complex flows and noise induced flows. LES computes the large resolved scales and also models the smallest scales. The turbulence model is incorporated by dividing the time and space varying flow parameters into two components, the resolved one  $\bar{f}$  and  $f'$ , the unresolved portion:

$$(x, t) = \bar{f}(x, t) + f'(x, t) \tag{7}$$

LES usages a filtering operation to separate these resolved scales from the unresolved scales. The filtered parameter is represented by an over bar [7]. The top-hat filter smooth both the fluctuations of the large-scale as well as those of small scales. The filtering operation whenever introduced to the Navier-Stokes equation, it results in:

$$\frac{\partial \bar{p}}{\partial \tau} + \nabla \cdot (\bar{\rho} \bar{U}) = 0 \tag{8}$$

$$\frac{\partial (\bar{\rho} \bar{U})}{\partial \tau} + \nabla \cdot (\bar{\rho} \bar{U} \bar{U}) - \nabla \cdot \nabla (\bar{\mu} \bar{U}) = -\nabla \bar{p} \tag{9}$$

$$\frac{\partial (\bar{\rho} \bar{e})}{\partial \tau} + \nabla \cdot (\bar{\rho} \bar{U} \bar{e}) - \nabla \cdot \nabla (\bar{\mu} \bar{e}) = -\bar{p} (\nabla \cdot \bar{U}) + \mu \left[ \frac{1}{2} (\nabla \bar{U} + \nabla \bar{U}^T) \right]^2$$

$$(10)$$

Nevertheless, the dissipative scales of motion are rectified poorly by LES. In a turbulent flow, the energy from the large resolved structures are passed on to the smaller unresolved structures by an inertial and an effective inviscid mechanism. This is called as energy cascade. Therefore, LES employs a sub-grid scale model to mimic the drain pertaining to this energy cascade. Most of these models are eddy viscosity models connecting the subgrid-scale stresses ( $\tau_{ij}$ ) and the resolved-scale rate of strain-tensor ( $\bar{S}_{ij}$ ),

$$\tau_{ij} - (\delta_{ij}/3) = -2\nu_T \bar{S}_{ij} \tag{11}$$

Where,  $\bar{S}_{ij}$  is the resolved-scale rate of strain tensor =  $(\partial \bar{u}_i / \partial x_j + \partial \bar{u}_j / \partial x_i) / 2$ .

In most of the circumstances it is supposed that all the energy received by the unresolved-scales are dissipated instantly. This is the equilibrium assumption, i.e., the small-scales are in equilibrium [7]. This simplifies the problem to a great extent and an algebraic model is found for the eddy viscosity:

$$\mu_{sgs} = \rho C \Delta^2 |\bar{S}| \bar{S}_{ij}, |\bar{S}| = (2\bar{S}_{ij} \bar{S}_{ij})^{1/2} \tag{12}$$

Here,  $\Delta$  is the grid size and is generally considered to be the cube root of the cell volume [7]. This model is termed as the Smagorinsky model and  $C$  is the Smagorinsky coefficient. In the current investigation, its value has been considered to be 0.2.

## VI. NUMERICAL PROCEDURES

### A. Numerical scheme and solution algorithm

The 3D compressible Navier-Stokes governing transport equations are discretized over an outline concerning finite volume method (FVM) through the SIMPLER algorithm. Here, the turbulent model utilized for large eddy simulation is Smagorinsky model, on account of its minimalism. The spatial derivatives like Laplacian and convective terms are computed by second order scheme based on Gauss theorem. Furthermore, the viscous terms are calculated by second order scheme. Additionally, the implicit second order scheme is utilized for time integration. The numerical fluxes are calculated by using Sweby limiter in central differencing (CD) scheme, which is a total variation diminishing (TVD) scheme. The central differencing (CD) is an unbounded second order scheme, while, the total variation diminishing (TVD) is a limited linear scheme. The developed solver is utilized to predict flow behaviours of the related flow variables pertaining to supersonic flow over an open cavity.

**B. Choice of grid size, time step and convergence criteria**

The computational domain is again decomposed into upper cavity and inside cavity region as illustrated in figure 2. The grid is refined at the regions near to the wall (where very high gradient is expected) to determine the behaviour of shear layer satisfactorily. A comprehensive grid-independence test is performed to establish a suitable spatial discretization, and the levels of iteration convergence criteria to be used. As an outcome of this test, the optimum number of grid points used for the final simulation, in the upper cavity region as  $360 \times 150 \times 1$  and those of in the inside cavity region as  $200 \times 150 \times 1$ . The grid spacing at the leading edge of the cavity denoted as  $\Delta X$ ,  $\Delta Y$  and  $\Delta Z$  being 5.0, 12.5, and 1.0, respectively. However, the total number of grid points is 81000 for this cavity. Corresponding time step chosen in the numerical simulation is  $10^{-6}$  seconds. Even though, it is tested with smaller grids of 128000 in numbers, it is witnessed that a finer grid structure does not change the results considerably.

The convergence in inner iterations is confirmed only when the condition  $\left| \frac{\phi - \phi_{old}}{\phi_{max}} \right| \leq 10^{-4}$  is fulfilled concurrently for all variables, where  $\phi$  represents the field variable at a grid point at the current iteration level,  $\phi_{old}$  stands for the corresponding value at the previous iteration level, and  $\phi_{max}$  is the maximum value of the variable at the current iteration level in the whole domain.

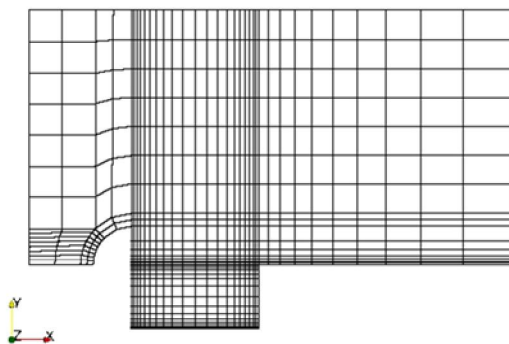


Figure 2. Computational grid of cavity with spoiler in X-Y Plane

**VII. RESULTS AND DISCUSSION**

The recirculation require to be reduced within the open cavity. Moreover, then o is reproduced owing to the flow over the said cavity need to be reduced. This can be attained by deploying a spoiler at the leading edge of the open cavity. The spoiler deployed in the present study is one-fourth part of a cylinder.

**A. Comparisons of velocity distributions with and without spoiler**

The velocity vectors, at an instant of time  $t = 0.1$  sec, for supersonic flow past an open cavity with and without the attachment of spoiler are revealed in the figure 3. The velocity vector indicates the recirculation within the open cavity. The flow performance past the open cavity with spoiler is unlike the open cavity flow without spoiler which may clearly be perceived from the velocity vectors. One shedding vortex is comprehended within the open cavity with spoiler at odds with two shedding vortices observed with in the open cavity without spoiler. The recirculation regimes of both the open cavities are quite different from each other. The velocity vectors relating to supersonic flow past the open cavity with and without the attachment of spoiler, at an additional instant of time  $t = 0.3$  sec, are also demonstrated in the figure 4. The distinctions in the flow behaviours may also be observed from both the stated figures portrayed at two different instants of times.

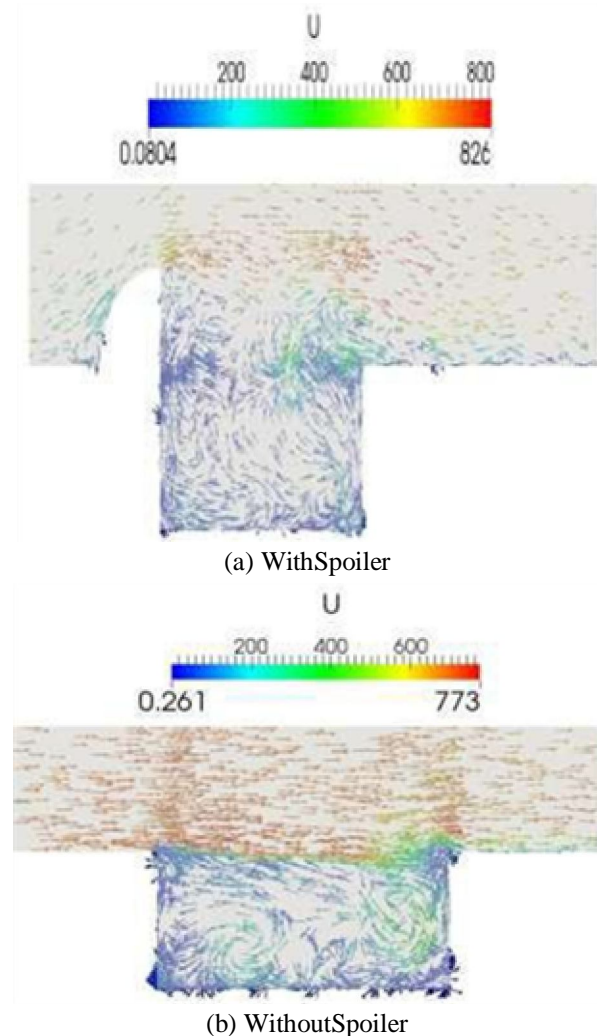


Figure 3. Velocity vector at instant of time,  $t = 0.1$  sec, with and without the use of spoiler



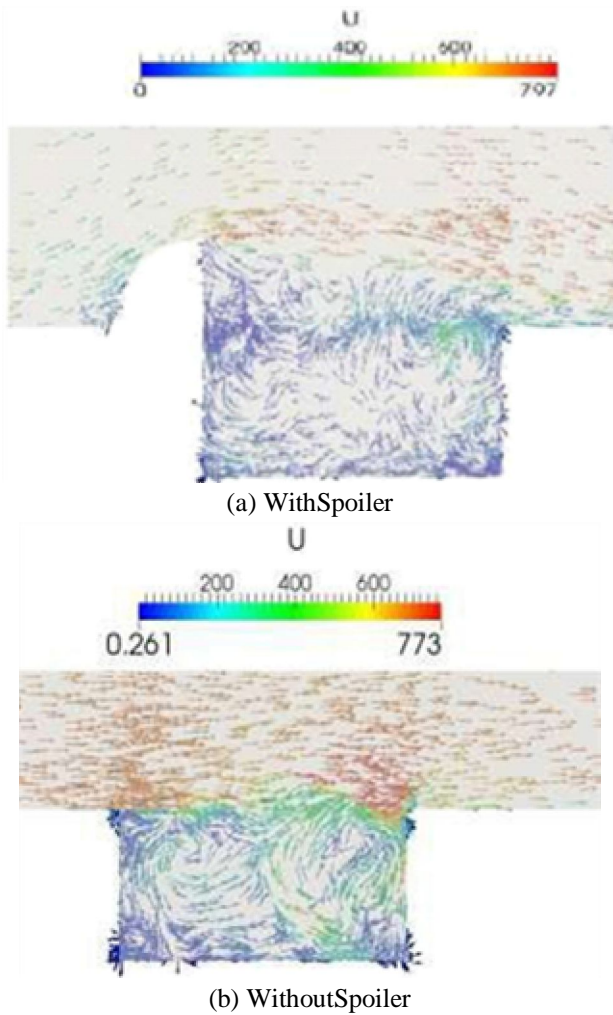


Figure 4. Velocity vector at instant of time, t = 0.3 sec, with and without the use of spoiler

**B. Comparisons of overall sound pressure level (OASPL) with and without spoiler**

The comparison of the OASPL (Overall Sound Pressure Level) distributions at the centreline of the aft wall of the open cavity has also been made. The OASPL is denoted as:

$$OASPL = 10 \log_{10} (\overline{p_d^2} / q^2) \tag{13}$$

Where, 
$$\overline{p_d^2} = \frac{1}{t_f - t_i} \int_{t_i}^{t_f} (p - \bar{p})^2 dt \tag{14}$$

$q$  is the acoustic sound reference level ( $= 2 \times 10^{-5}$  Pa)  
 $\bar{p}$  is the time-averaged static pressure  
 $t_f$  and  $t_i$  are the initial and final times, respectively

The OASPL distribution at the centreline of the aft wall of the open cavity with spoiler has been compared with

that of without the attachment of spoiler. The comparison of both the said cases are presented in the figure 5. It is pragmatic that the OASPL is suppressed by approximately 18 dB and 14 dB at both aft and front walls of the stated open cavity, respectively. In addition, the OASPL distribution as observed at the centreline of the aft wall of the open cavity with spoiler attachment, remains almost uniform throughout.

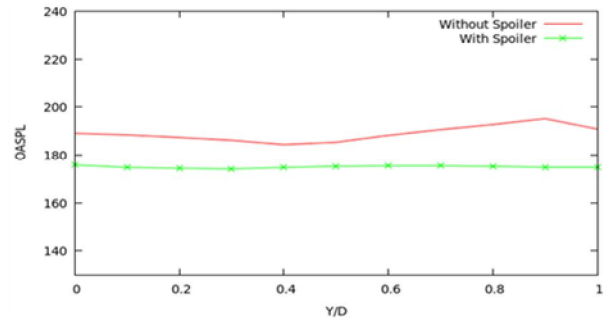


Figure 5. OASPL distribution at the centreline of the aft wall of the cavity with and without the use of spoiler

**VIII. CONCLUSION**

In the present investigation, the numerical simulation has been accomplished for supersonic flow past an open cavity with and without the attachment of spoiler. The open cavity has length-to-depth ratio of 2 in addition Mach number of the free-stream is 2.0. The simulation is conducted with LES based on Smagorinsky model. The numerical results are obtained in the form of both cavity flow-field analysis as well as the aeroacoustic analysis epitomised by the overall sound pressure level at the centreline of the aft wall of the open cavity. The LES model is capable to ascertain all the core flow structures of the open cavity. The overall sound pressure level at the centreline of the aft wall of the open cavity with spoiler is compared with that of without the spoiler. There is both qualitative and quantitative agreement between the two. Nevertheless, with the attachment of spoiler, the sound pressure level is reduced by nearly 18 dB at the aft wall and also decreased by about 14 dB at the front wall of the stated open cavity. The trends of predictions for both the cavities are similar and therefore are comparable. In addition, the recirculation within the open cavity is also suppressed by use of spoiler which is also observed from the velocity vector. As a whole, in this investigation, a three-dimensional model is established for an open cavity and a spoiler is attached at its leading edge to study the flow structures and to suppress the recirculation within the open cavity. Furthermore, the overall sound pressure level at the centreline of the aft wall of the open cavity is also witnessed to be reduced.

**IX. ACKNOWLEDGMENT**

The author would like to thank the editor and the reviewers for extending their constructive remarks, valuable time and contributions for providing insightful reviews to the research article.

## REFERENCES

- [1] Heller, H. H., Holmes, D. G., & Covert, E. E. (1971). Flow-induced pressure oscillations in shallow cavities. *Journal of sound and Vibration*, 18(4), 545-553.
- [2] Tam, C. K., & Block, P. J. (1978). On the tones and pressure oscillations induced by flow over rectangular cavities. *Journal of Fluid Mechanics*, 89(02), 373-399.
- [3] Kaufman, I. I., Louis, G., Maciulaitis, A., & Clark, R. L. (1983). Mach 0.6 to 3.0 flows over rectangular cavities (No. AFWAL-TR-82-3112). Air force wright aeronautical labs wright-patterson AFB, OH.
- [4] Sweby, P. K. (1984). High resolution schemes using flux limiters for hyperbolic conservation laws. *SIAM journal on numerical analysis*, 21(5), 995-1011.
- [5] Rizzetta, D. P. (1988). Numerical simulation of supersonic flow over a three-dimensional cavity. *AIAA journal*, 26(7), 799-807.
- [6] Anderson, J. D., & Wendt, J. F. (1995). *Computational fluid dynamics* (Vol. 206). New York: McGraw-Hill.
- [7] Piomelli, U. (1999). Large-eddy simulation: achievements and challenges. *Progress in Aerospace Sciences*, 35(4), 335-362.
- [8] Hamed, A., Das, K., & Basu, D. (2004). Numerical simulations of fluidic control for transonic cavity flows. *AIAA Paper*, 429, 2004.
- [9] Li, W., Nonomura, T., Oyama, A., & Fujii, K. (2010). LES Study of Feedback-loop Mechanism of Supersonic Open Cavity Flows. *AIAA paper*, 5112, 2010.
- [10] Vijayakrishnan, K. (2014) Unsteady RANS computations of supersonic flow over two dimensional cavity using OpenFOAM-A validation study. *AIAA* 2014.
- [11] Sousa, R. G., et al. (2016). Lid-driven cavity flow of viscoelastic liquids. *Journal of Non-Newtonian Fluid Mechanics*, 234, 129-138, 2016.
- [12] Tuerke, F., Pastur, L. R., Sciamarella, D., Lusseyran, F., & Artana, G. (2017). Experimental study of double-cavity flow. *Experiments in Fluids*, 76, 2017.